

The Dependence of the Age Parameter from EAS Size and Zenith Angle of Incidence

A.A. Chilingarian, G.V. Gharagozyan*, S.S. Ghazaryan, G.G. Hovsepyan,
E.A. Mamidjanyan, L.G. Melkumyan, S.H. Sokhoyan
Yerevan Physics Institute, Cosmic Ray Division, Armenia

The quality of the MAKET-ANI detector installation in view of the uniformity of the registration efficiency is demonstrated. Based on a data sample collected by the MAKET-ANI array in the period of June 1997 - March 1999, the dependencies of the age parameter on the zenith angle and the EAS size ($10^5 - 10^7$) are studied. The variation of the age parameter with the shower size can be approximately related to the elongation rate.

1 Introduction

The lateral distribution of the charged particle component of extensive air showers (EAS) carries information about the height of maximum of the EAS development. In NKG type parameterizations of the lateral distribution this information is associated with the so-called age parameter s , originally introduced by the analytic description of purely electromagnetic cascades for characterizing the actual stage of the EAS development.

In EAS experiments this parameter is usually extracted from fitting the distribution measured on observed level, assuming that this lateral parameter reflects the actual longitudinal EAS stage. Investigations of the parameter s have been performed on various altitudes, with the aim to gain information on the longitudinal EAS development and on the composition of primary cosmic rays [1-7]. For example, from the analysis of the zenith angle dependence of the average value of s it has been concluded that the mass composition gets either heavier primary energies larger than 10^{15} eV or the multiplicity of secondary particle production in hadronic interactions is unexpectedly increasing. In the present contribution experimental age distributions, dependent on the zenith angle θ of EAS incidence and of the shower size N_e as extracted from an actual data set of the MAKET-ANI array, are communicated. As compared to earlier results [4] the statistical accuracy of the data is considerably improved thanks to various modernizations of the installation [5]. The variation of the age parameter with the observation depth X is considered by a simplified approach.

2 Some characteristics of the data selection

With an effective running time of ca. 8000 h the array triggered for $2.6 \cdot 10^6$ showers. From this set 177066 showers have been selected with following criteria: $N_e \geq 1 \times 10^5$, $\theta < 45^\circ$, $0.3 \leq s \leq 1.7$. The procedures of data selection and further analyses are given in Ref. [5]. The effective area for EAS registration, varying from $28 \cdot 14m^2$ for $N_e \geq 10^5$ to $64 \cdot 32m^2$ for $N_e \geq 10^6$. With Monte Carlo simulations and experimental considerations of the angular accuracy following uncertainties of the reconstructed EAS parameters were obtained: core location: $\delta R \simeq 1.5$ m, $\delta N_e \simeq 15\%$ for $N_e < 10^6$, $\delta N_e \simeq 10\%$ for $N_e > 10^6$, $\delta s \simeq 7\%$, $\delta\theta < 1.5^\circ$ and $\delta\varphi < 5^\circ$.

Figures 1 and 2 display the good uniformity of the EAS registration; the maximum intensity results

*corresponding author: gagik@crdlx5.yerphi.am

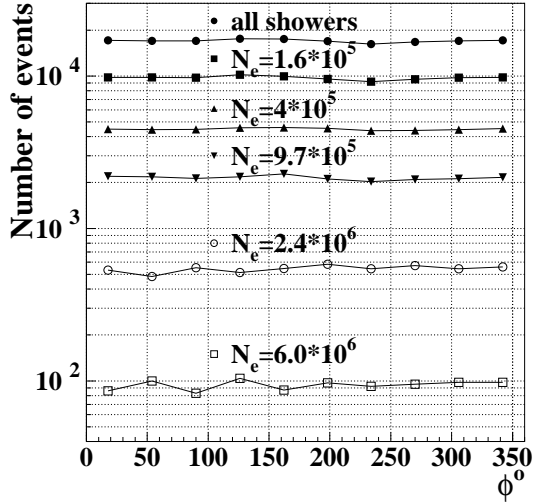


Figure 1: Distributions of the EAS azimuth angles φ for different EAS sizes.

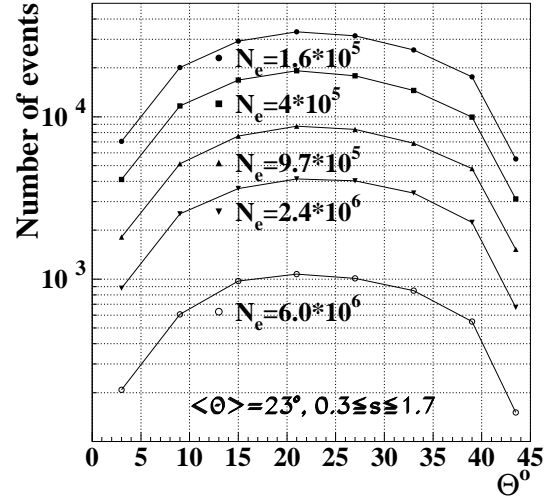


Figure 2: Distributions of the EAS zenith angles for different EAS sizes.

from the zenith angle of $\bar{\theta} \simeq 23^\circ$. For more detailed analyses the EAS sample is divided in three classes: "young" showers with $0.3 < s < 0.8$, "mature" showers with $0.8 < s < 1.1$, and "old" showers with $1.1 < s < 1.7$.

Figure 3 display the uniform efficiency of the age selection of the procedures.

3 Age parameter distributions

The distributions of the age parameter values for various EAS sizes are shown in Figure 4, displayed for different ranges of the zenith angles of EAS incidence. The distributions get narrower and show decreasing variances with increasing N_e in agreement with Ref. [1]. This can be understood that small size showers penetrating in the deeper atmosphere show larger fluctuations in s . The average age is slightly, but systematically shifted to higher values with increasing atmospheric depth.

For a consideration of the dependence of the average age from N_e and zenith angle a finer binning of the total angular range has been applied. As examples in Figure 5 the dependence of the mean age is shown for selected angular bins (representing "vertical", "inclined" and all showers). The results are compared with the Norikura data [1], which show similar tendencies, but shifting the global features

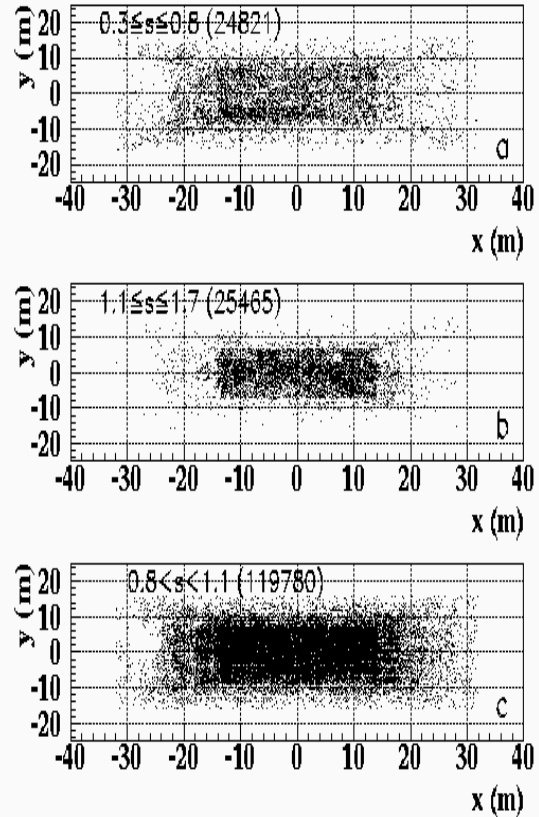


Figure 3: Distribution of the core locations of different age classes of showers.

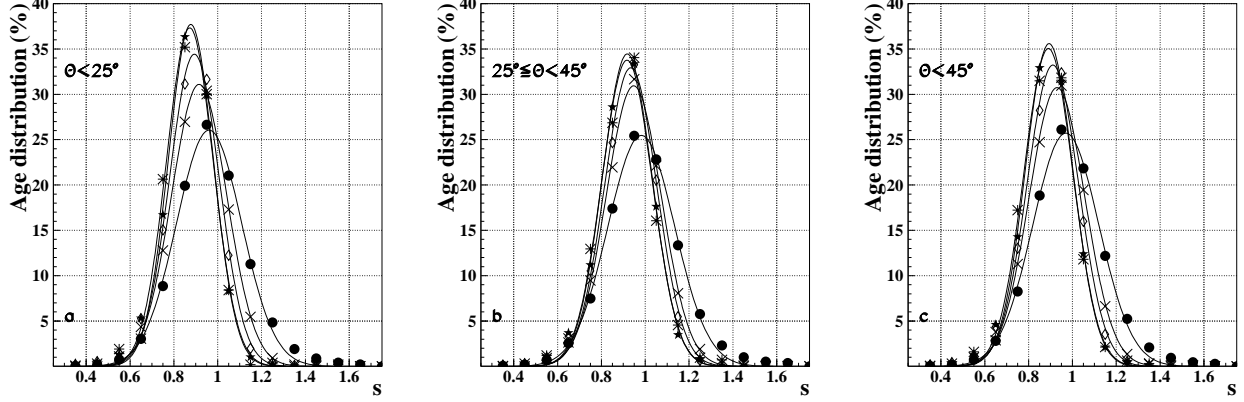


Figure 4: Age parameter distributions for various EAS sizes and angular ranges of EAS incidence: a- vertical, b- inclined, c- all showers. $N_e = \bullet - 1.6 \cdot 10^5$, $\times - 4.0 \cdot 10^5$, $\diamond - 9.7 \cdot 10^5$, $\star - 2.4 \cdot 10^6$, $\ast - 6.0 \cdot 10^6$.

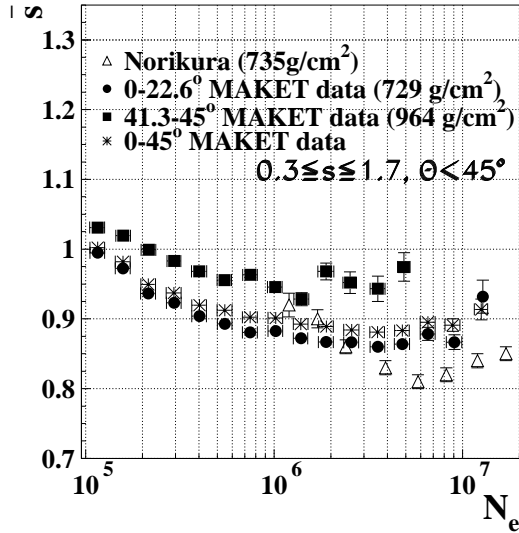


Figure 5: \bar{s} dependence of the shower size.

to larger and younger EAS. It is not clear if this finding is due methodical effects of different evaluation procedures in both experiments. The results of MAKET-ANI agree with the observations Ref. [7], if taking into account the different observation levels, but disagrees with the data of the MSU group [3], the latter claiming an almost constant mean age for EAS of $N_e = 10^5 - 10^6$. There are results of EAS simulations, based on the QGSJET model as generator [8], which show fair agreement [9].

The variation of the average age is affected by the primary energy spectrum, by the change of the chemical composition and the hadronic interaction characteristics, governing the EAS development. As long as there is no noticeable change, the average depth of the shower maximum is expected to be increasing monotonously. Hence the shallow slope of the average age for $N_e > 10^6$ may indicate

a faster EAS development due to an increasing multiplicity of the secondary production and a heavier composition, respectively.

4 EAS size spectra of different ages

Figure 6 shows the integral size spectra for "young", "mature" and "old" showers for two different angular ranges of shower incidence. While the young and mature shower spectra exhibit the knee feature, a knee is not evident for old showers, which show obviously a different variation with the shower size. This behavior results also from an analysis of KASCADE data classified along various types of primaries by methods of advanced statistical analysis [10]. The old showers are tentatively associated to iron-like showers with a different knee position.

The lower part of Figure 6, taken from Ref. [2], where the showers have been classified by an analysis

of the appearance of the shower core, shows a good consistency. There are, however some differences with the Tien-Shan data (given in Ref.[11]). While the slopes are identical for mature showers and equal for old showers, the young showers do not display a knee in the data of Ref. [11]. Whether these differences can be explained by the particular analysis procedures, is not yet clarified.

Figure 7 presents the spectra for different values of the age parameters and characterized by the spectral indices given Table 2 (extracted by the procedures of Ref. [12]). With increasing age values the spectral slope gets flatter before the knee as also evidenced by the KASCADE data [13]. Old showers exhibit a quite different slope.

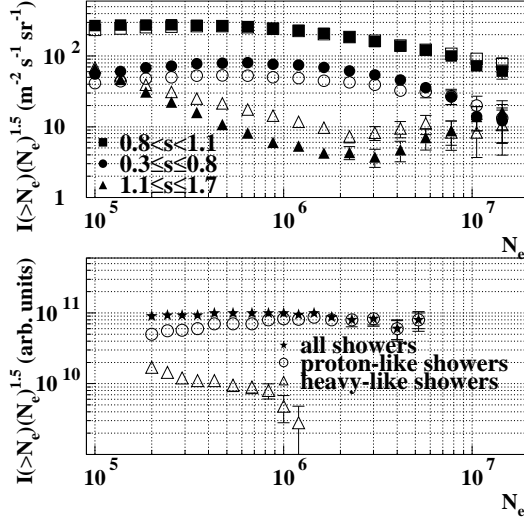


Figure 6: Integral EAS size spectra for two different ranges of the zenith angles (closed symbols: $\theta = 0^\circ - 25^\circ$, open symbols: $\theta = 25^\circ - 45^\circ$ for young, mature and old showers. The lower part of the figure is taken from Ref. [2] for comparison.

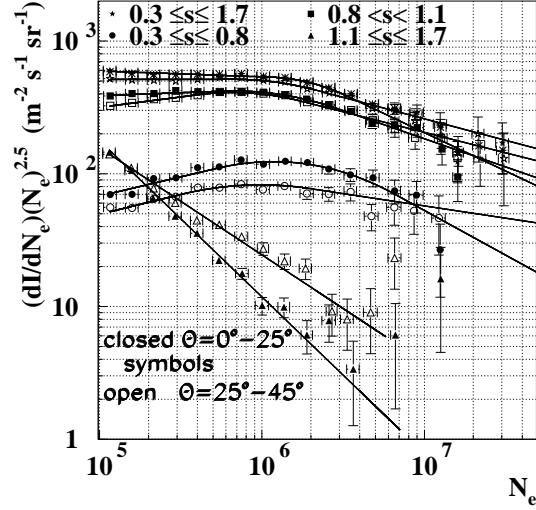


Figure 7: Differential EAS size spectra for different angular and age ranges.

Table 1: Average age values and variances for different zenith angles ($\theta < 25^\circ$, $25^\circ \leq \theta < 45^\circ$, $\theta < 45^\circ$) and EAS sizes together with the values of the parameters A and $s(\theta = 0)$ of the parameterization of the $\sec \theta$ dependence.

N_e	$\theta < 25^\circ$		$25^\circ \leq \theta < 45^\circ$		$\theta < 45^\circ$		A	$s(0)$
	\bar{s}	σ_s	\bar{s}	σ_s	\bar{s}	σ_s		
1.6×10^5	0.96	0.15	0.98	0.15	0.97	0.15	$0.126 \pm .002$	$0.968 \pm .001$
4.0×10^5	0.92	0.13	0.95	0.13	0.93	0.13	$0.194 \pm .004$	$0.902 \pm .005$
9.7×10^5	0.89	0.11	0.93	0.12	0.91	0.12	$0.241 \pm .006$	$0.872 \pm .007$
2.4×10^6	0.88	0.10	0.92	0.11	0.89	0.11	$0.274 \pm .008$	$0.855 \pm .009$
6.0×10^6	0.87	0.11	0.92	0.12	0.89	0.11	$0.316 \pm .2$	$0.852 \pm .032$
$\geq 10^7$	0.93	0.14	0.96	0.14	0.94	0.14	$0.161 \pm .002$	$0.934 \pm .001$

Table 2: Spectral slopes ($dI/DN_e \propto N_e^{-\gamma}$) and knee positions for different ranges of the age parameter values.

θ	s	γ_1	γ_2	$\log(N_e^{knee})$
$0^\circ - 25^\circ$	0.3 - 1.7	2.54 ± 0.03	3.08 ± 0.03	6.30
	0.8 - 1.1	2.45 ± 0.03	2.92 ± 0.07	6.13
	0.3 - 0.8	2.21 ± 0.03	3.17 ± 0.14	6.31
	1.1 - 1.7	3.68 ± 0.08		
$25^\circ - 45^\circ$	0.3 - 1.7	2.50 ± 0.02	2.82 ± 0.04	6.08
	0.8 - 1.1	2.34 ± 0.03	2.81 ± 0.05	5.93
	0.3 - 0.8	2.20 ± 0.02	2.70 ± 0.07	5.91
	1.1 - 1.7	$3.31 \pm .07$		

5 Variation of the age with the observation depth

Figure 8 shows the dependence of the mean age $\bar{s}(\theta)$ of particular EAS sizes from the zenith angle θ , as linear dependence from $\sec\theta$.

The parameters $\bar{s}(0)$ and A, adjusted to the $\sec\theta$ dependence are given in Table 1.

With increasing N_e the slope A increases while $\bar{s}(0)$ is decreasing. There is a good agreement with the values of Ref. [1] obtained for $N_e = 2.4 \cdot 10^6$.

The values averaged over all EAS sizes are $A = 0.161 \pm 0.002$ and $\bar{s}(0) = 0.934 \pm 0.001$. With the approximate relation $\sec\theta = X/X_v$ where X_v is depth of the observation level and X the transverse atmospheric thickness (grammage) A can be related to the change $d\bar{s}/dX$ of the average age with X. With the average value of A inferred from the data for the observation level $X_v = 700 \text{ g/cm}^2$ a value $d\bar{s}/dX = 2.3 \cdot 10^{-4} \text{ cm}^2/\text{g}$. This result can be compared with $d\bar{s}/dX = 3.4 \cdot 10^{-4} \text{ cm}^2/\text{g}$ given in [1]. A compilation [1] of the data from the literature yields a range $d\bar{s}/dX = (1.9 - 4.3) \cdot 10^{-4} \text{ cm}^2/\text{g}$. Associating the depth of the shower maximum X_m with $\bar{s} = 1$, we reach the relation

$$\bar{s} - 1 = \frac{d\bar{s}}{dX} \cdot (X - X_m), \quad (1)$$

Thus an evaluation of the N_e dependence of $\Delta X = (X - X_m)$ carries some information about the elongation rate, as already indicated by Linsley [14].

6 Concluding Remarks

The present results deduced from the data of the MAKET-ANI array are in good agreement with theoretical expectations. The analyses reveal that:

- Average age parameter gradually decreases with increasing shower size from 10^5 to 10^6 , and for

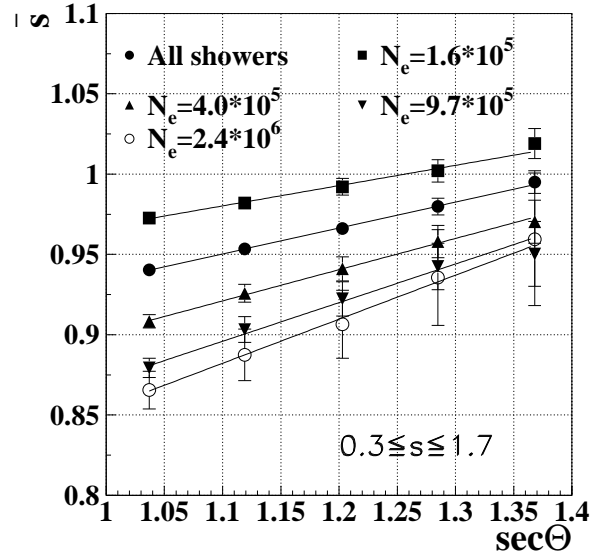


Figure 8: The dependence of the mean age \bar{s} from the zenith angle of EAS incidence for various shower sizes.

$N_e > 10^6$ it becomes almost constant.

- The knee of "young" showers is sharper than knee of the all particle spectra.
- The size spectra classified by different ages show different attenuation.
- The change of age parameter with the zenith angle of EAS incidence can be related to the change of the EAS maximum with N_e .

Acknowledgment

The report is based on scientific results of the ANI collaboration. The MAKET-ANI installation on Mt.Aragats has been setup as a collaboration project of the Yerevan Physics Institute (Armenia) and the Lebedev Physics Institute (Moscow). The continuous contributions and assistance of the Russian colleagues in operating of the installation and in the data analyses are gratefully acknowledged. In particular, we thank Prof. S. Nikolski and Dr. V. Romakhin for their encouraging interest to this work and useful discussions.

We would like to thank Prof. Dr. H. Rebel pointing on the importance of the elongation rate estimation, Dr. A. Haungs and Dr. Kh. Sanosyan for useful remarks. Corrections and suggestions made by Dr. S. Ostapchenko are highly appreciated. The assistance of the Maintenance Staff of the Aragats Cosmic Ray Observatory in operating the MAKET-ANI installation is highly appreciated. The work has been partly supported by the ISTC project A116.

References

- [1] S. Miayke et al., Proc. 16th ICRC (Kyoto) **13** (1979) 171
S. Miayke et al., Proc. 17th ICRC (Paris) **11** (1981) 293
B.S. Acharya et al., Proc. 17th ICRC (Paris) **9** (1981) 162
- [2] J. Kempa and M. Samorski, J.Phys. G: Nucl. Part. Phys. **24** (1998) 1039
- [3] G.B. Khristiansen et al., Proc. AS USSR, Phys. **35** (1971), 2107 (in Russian)
G.B. Khristiansen et al., Proc. 17th ICRC (Paris) **6** (1981) 39
N.N. Kalmykov et al., Proc. 25th ICRC (Durban) **6** (1997) 277
- [4] V.V. Avakian et al., Soviet J. Nucl. Phys. **56** (1993) 183 (in Russian)
- [5] G.V. Gharagozyan for the ANI collab., Proc. of the Workshop ANI 98, eds. A.A. Chilingarian, H.Rebel, M. Roth, M.Z. Zazyan, FZKA 6215, Forschungszentrum Karlsruhe 1998, p.51
- [6] L.G. Melkumyan for the ANI collab., ANI Workshop 1999, these proceedings
- [7] K. Asakimori et al., Proc. 17th ICRC (Paris) **11** (1981) 301
T. Hara et al., Proc. 17th ICRC (Paris) **6** (1981) 52
K. Asakimori, Proc. 21st ICRC (Adelaide) **3** (1990) 129
- [8] N.N. Kalmykov, S.S. Ostapchenko and A.J. Pavlov, Nucl. Phys. B **52R** (1997) 17
- [9] S.S. Ostapchenko, private communication
- [10] A. Vardanyan et al. - KASCADE collaboration, these proceedings
- [11] S.I. Nikolsky, Proc. 25th ICRC (Durban) **6** (1997) 105
- [12] S.H. Sokhoyan et al., these proceedings
- [13] R. Glasstetter et al. - KASCADE collaboration, Proc. 25th ICRC (Durban) **6** (1997) 157
- [14] J. Linsley, Proc. 15th ICRC (Plovdiv) **12** (1977) 89